Endocrine (2019) 64:393–405
https://doi.org/10.1007/s12020-018-1796-9

ORIGINAL ARTICLE

Limited short-term effects on human prostate cancer xenograft growth and epidermal growth factor receptor gene expression by the ghrelin receptor antagonist [D-Lys^3]-GHRP-6

Michelle L. Maugham[1,2,3,4] · Inge Seim[1,2,3,5] · Patrick B. Thomas[1,2,3] · Gabrielle J. Crisp[1,2,3] · Esha T. Shah[1,2,3] · Adrian C. Herington[1,2] · Laura S. Gregory[4] · Colleen C. Nelson[2] · Penny L. Jeffery[1,2,3] · Lisa K. Chopin[1,2,3]

Received: 20 June 2018 / Accepted: 17 October 2018 / Published online: 2 November 2018

Abstract

Purpose The ghrelin axis regulates many physiological functions (including appetite, metabolism, and energy balance) and plays a role in disease processes. As ghrelin stimulates prostate cancer proliferation, the ghrelin receptor antagonist [D-Lys^3]-GHRP-6 is a potential treatment for castrate-resistant prostate cancer and for preventing the metabolic consequences of androgen-targeted therapies. We therefore explored the effect of [D-Lys^3]-GHRP-6 on PC3 prostate cancer xenograft growth.

Methods NOD/SCID mice with PC3 prostate cancer xenografts were administered 20 nmoles/mouse [D-Lys^3]-GHRP-6 daily by intraperitoneal injection for 14 days and tumour volume and weight were measured. RNA sequencing of tumours was conducted to investigate expression changes following [D-Lys^3]-GHRP-6 treatment. A second experiment, extending treatment time to 18 days and including a higher dose of [D-Lys^3]-GHRP-6 (200 nmoles/mouse/day), was undertaken to ensure repeatability.

Results We demonstrate here that daily intraperitoneal injection of 20 nmoles/mouse [D-Lys^3]-GHRP-6 reduces PC3 prostate cancer xenograft tumour volume and weight in NOD/SCID mice at two weeks post treatment initiation. RNA-sequencing revealed reduced expression of epidermal growth factor receptor (EGFR) in these tumours. Further experiments demonstrated that the effects of [D-Lys^3]-GHRP-6 are transitory and lost after 18 days of treatment.

Conclusions We show that [D-Lys^3]-GHRP-6 has transitory effects on prostate xenograft tumours in mice, which rapidly develop an apparent resistance to the antagonist. Although further studies on [D-Lys^3]-GHRP-6 are warranted, we suggest that daily treatment with the antagonist is not a suitable treatment for advanced prostate cancer.

Keywords Prostate cancer · Ghrelin · Ghrelin receptor antagonist · [D-Lys^3]-GHRP-6 · PC3 · Xenograft

Introduction

The peptide hormone ghrelin is a recognised mediator of numerous physiological processes, including appetite

Electronic supplementary material The online version of this article (https://doi.org/10.1007/s12020-018-1796-9) contains supplementary material, which is available to authorized users.

✉ Lisa K. Chopin
l.chopin@qut.edu.au

[1] Ghrelin Research Group, Institute of Health and Biomedical Innovation, Translational Research Institute and School of Biomedical Sciences, Queensland University of Technology, Brisbane, QLD, Australia

[2] Australian Prostate Cancer Research Centre - Queensland, Princess Alexandra Hospital, Institute of Health and Biomedical Innovation, Translational Research Institute, Queensland University of Technology, Brisbane, QLD, Australia

[3] Comparative and Endocrine Biology Laboratory, Institute of Health and Biomedical Innovation, Translational Research Institute, Queensland University of Technology, Brisbane, QLD, Australia

[4] Skeletal Biology and Forensic Anthropology Research Laboratory, Cancer Program, School of Biomedical Sciences, Institute of Health and Biomedical Innovation, Translational Research Institute, Queensland University of Technology, Brisbane, QLD, Australia

[5] Integrative Biology Laboratory, College of Life Sciences, Nanjing Normal University, Nanjing, Jiangsu, China

regulation [1, 2], insulin release [3], energy balance, and adipogenesis [4]. Ghrelin, therefore, has emerged as a target for the treatment and prevention of obesity and metabolic syndrome [5, 6]. Furthermore, there is now close to two decades of evidence for a role of ghrelin in cancer [7–9]. In prostate cancer, ghrelin treatment increases the proliferation of the PC3 and LNCaP human prostate cancer cell lines *in vitro* [10]. Additionally, prostate cancer cell lines express components of the ghrelin axis, including its receptor GHSR1a (*GHSR*) and the ghrelin activating enzyme ghrelin *O*-acyl transferase (GOAT; encoded by *MBOAT4*) [9, 10]. The insulin-regulated ghrelin (*GHRL*) isoforms in2c-ghrelin [11] and in1-ghrelin [11] are highly expressed relative to the wild-type ghrelin isoform in prostate cancer cell lines and clinical tumours [10, 11]. Many of the effects of ghrelin, including appetite regulation, are mediated by its cognate receptor, the growth hormone secretagogue receptor 1a (GHSR1a), which is a G protein-coupled receptor (GPCR) [3]. GPCR-ligand interactions are common therapeutic targets for a number of disease states [12]. The GHSR1a has been targeted to manipulate the ghrelin axis [13, 14] as ghrelin resistance is linked with obesity [15, 16]. Being overweight or obese is a risk factor for many cancers [17] and is associated with progression of prostate, endometrial, breast, and gastrointestinal cancer [18–21]. Although ghrelin and GHSR antagonists have not been approved as treatments for excessive appetite and obesity, the metabolic and proliferative effects of ghrelin in cancer could prove fruitful therapeutic targets [8]. In particular, the inhibition of ghrelin signalling through the GHSR1a by ghrelin antagonists may be effective in treating cancers fuelled by hypernutrition [22, 23].

Here, we studied the effect of the well-characterised and commercially-available [24] ghrelin receptor antagonist [D-Lys^3]-GHRP-6 on prostate tumour growth *in vivo*. [D-Lys^3]-GHRP-6 is a potent, peptidic GHSR1a antagonist [24]. It also antagonises other receptors, including the chemokine G protein-coupled receptors CXCR4 [25] and CCR5 [26], however, at much lower potency.

Materials and methods

Cell culture

Human prostate cancer cell lines were obtained from the American Type Culture Collection (ATCC, Manassas, VA, USA). The PC3 prostate cancer cell line was cultured in Roswell Park Memorial Institute 1640 medium (RPMI-1640) and supplemented with 10% (v/v) fetal bovine serum (FBS) (Thermo Fisher Scientific, Waltham, MA, USA), 50 units/ml penicillin, and 100 µg/ml streptomycin (Invitrogen, Carlsbad, CA, USA). All cells tested negative for *Mycoplasma*. The cell line was authenticated by the QUT Genomics Research Centre.

Cell proliferation assays

To determine the effect of [D-Lys^3]-GHRP-6 (Sigma-Aldrich, St-Louis, MO, USA) on PC3 prostate cancer cell line growth *in vitro* Wst-1 (Roche Applied Science, Penzberg, Germany) and Incucyte Zoom proliferation assays were performed. Cells were plated at 2×10^4 cells per well in a 96 well plate, left overnight, then treated with a range of concentrations of [D-Lys^3]-GHRP-6 (0–10 µM, Sigma Aldrich) daily for three days. Wst-1 cell proliferation reagent agent was added to cells grown in 96 well plates (Thermo Fischer Scientific, Waltham, MA, USA) in phenol-red free media after 5 days, incubated for 1.5 h and absorbance measured using a Fluostar Omega (BMG LABTECH, Ortenberg, Germany) plate reader at 450 nm with a reference wavelength of 650 nm. For the IncuCyte ZOOM (Essen Bioscience, Ann Arbor, MI, USA) proliferation method, cells in 96 well plate Image lock 96 well plates (Essen Bioscience) were placed in the IncuCyte ZOOM incubator on the second day after the first treatment with [D-Lys^3]-GHRP-6 and images captured at 10× magnification every two hours and phase contrast was used by the instrument to determine percent confluency. All experiments were performed in triplicate with at least three independent repeats.

[D-Lys^3]-GHRP-6 in in vivo subcutaneous prostate cancer xenograft growth

In order to determine the effect of the ghrelin antagonist [D-Lys^3]-GHRP-6 on prostate cancer cell line xenograft growth, NOD.CB17-*Prkdc*^{scid}/Arc (NOD/SCID) mice (Jackson Laboratory; supplied by Animal Resource Centre, Murdoch, WA, Australia) received a subcutaneous injection of 1×10^6 PC3 cells into the left flank. The PC3 cells were diluted 1:1 in growth factor-reduced, phenol red-free Matrigel (Corning, NY, USA). Ethical approval was granted from the University of Queensland and Queensland University of Technology Animal Ethics Committees (TRI/QUT/087/14/NHMRC). Mice were housed under pathogen-free conditions in individually-ventilated cages at a room temperature of 20–23 °C, with a 12-h light-dark cycle [27].

Tumours were allowed to grow until a volume of approximately 100 mm^3 was reached, at which point mice were divided into two experimental groups. Mice then received daily intraperitoneal (i.p.) injections of 20 nmoles/mouse of [D-Lys^3]-GHRP-6 (Sigma-Aldrich) ($n = 4$) or PBS control ($n = 5$) for 14–18 days (ethical endpoint set at a tumour size of 1000 mm^3). Tumour volume was calculated by measuring subcutaneous tumour length and width twice

weekly using digital calipers (ProSciTech, Kirwan, QLD, Australia) and the equation 'tumour volume = (length × width^2)/2' [28]. At the end of the experiment, mice were euthanised using 70% carbon dioxide followed by cervical dislocation. Wet tumour weight and volume were measured and the excised tumour was divided into two, with half being formalin fixed and paraffin embedded for histology and the remaining half snap frozen and stored at −80 °C until required for gene expression analysis. A second *in vivo* study was performed to assess the effects of a longer time timepoint and larger dose of ghrelin receptor antagonist. In this experiment, 20 nmoles ($n = 11$) or 200 nmoles/mouse ($n = 10$) [D-Lys^3]-GHRP-6 (Sigma-Aldrich), or PBS control ($n = 11$) was administered by i.p. injection for 18 days once tumours reached approximately 100 mm^3, as described above.

RNA extraction from tissues

To extract RNA from tissues, TRIzol reagent (Life Technologies, Carlsbad, CA, USA) (1 mL per 50–100 mg tissue) and an RNeasy Mini Kit (QIAGEN, Hilden, Germany) were used to extract and purify RNA from snap frozen PC3 xenograft tumour tissue from mice treated with [D-Lys^3]-GHRP-6 or PBS (control). RNA was quantified using a NanoDrop ND-1000 spectrophotometer (Thermo Fisher Scientific) and stored at −80 °C. RNA was considered high quality (and suitable for use) if the 260/280 ratio was 1.9–2.1 and the 260/230 ratio was >1.5.

RNA-sequencing and analysis

RNA purity was assessed using an Agilent 2100 Bioanalyzer (Agilent, Santa Clara, CA, USA) and RNA was used for RNA-seq if the RNA Integrity Number (RIN) was >7. Strand-specific RNA-seq was performed by Macrogen (Seoul, South Korea). A TruSeq stranded mRNA library (Illumina, San Diego, CA, USA) was constructed and RNA-seq performed (130 million reads) on a HiSeq 2500 instrument (Illumina) to generate 101 bp paired-end reads. Preprocessing of raw FASTQ reads, including elimination of contamination adapters, was performed with scythe v0.994 (https://github.com/vsbuffalo/scythe). Human (xenograft tumour; the graft) and mouse (the host) RNA-seq reads were separated using Xenome [29] on the trimmed FASTQ files.

Paired-end human FASTQ files were aligned to the human genome (UCSC build hg19) using the spliced-read mapper TopHat (v2.1.1) [30] and reference gene annotations to guide the alignment. Raw gene counts were computed from TopHat-generated BAM files using featureCounts v1.4.6-p5 [31], counting coding sequence (CDS) features of the UCSC hg19 gene annotation file (gtf). FeatureCounts output files were analysed using the R programming language (v3.2.3). Briefly, raw counts were normalised by trimmed mean of *M*-values (TMM) correction [32, 33]. Library size-normalised read counts (per million; CPM) were subjected to variance-based filtering using the R package 'genefilter' v1.56.0 [34], with default settings, to remove genes that exhibited little variation across all samples. Differentially expressed genes were identified using the *voom* function (variance modelling at the observation-level) in the R package 'limma' v3.22.1 (Linear Models for Microarray Data) [35, 36]; with trend = TRUE for the eBayes function and correction for multiple testing (Benjamini-Hochberg false discovery rate and *P* value cut-off set to 0.05). Genes with at least a 2.0 absolute fold-change difference in expression between xenografts from mice treated with [D-Lys^3]-GHRP-6 or PBS control were defined as differentially expressed. Detailed gene annotations were obtained by querying Ensembl with the R/Bioconductor package 'biomaRt' [37].

To identify gene association networks in [D-Lys^3]-GHRP-6-treated xenograft tumours, differentially expressed genes were mapped onto STRING v10 [38, 39], using the R package 'Stringdb' v1.18.0 [40] (with score_threshold = 400), and visualised with iGraph [41]. STRING integrates functional annotation data—relationships between proteins that likely contribute to a common biological purpose. To assess network structure, we utilised the iGraph community algorithm Waltrap, reported to perform well on small networks [42]. Employing a 2.0-fold change and P value ≤ 0.05 cutoff, genes induced or repressed by [D-Lys^3]-GHRP-6 administration were indicated in the network (an in-house R script was used to allow custom colouring). Proteins in a network without connections were not shown. The expected vs. observed protein interactions and associated *P*-value were calculated based on a random background model [39] (implemented via *get_summary* in the 'Stringdb' R package).

Histology and immunohistochemistry

Excised tissues for histology were fixed in 4% paraformaldehyde (Electron Microscopy Sciences, Hatfield, PA), embedded in paraffin or snap frozen in OCT compound (VWR Prolab, Tingalpa, QLD, Australia), and stored at −80 °C. Frozen sections were cut (6–10 µm) using a Leica CM1850 cryotome (Leica Biosystems, Wetzlar, Germany), picked up onto warm charged slides, air-dried for one hour to overnight and stored at −80 °C. Before staining, sections were fixed in ice-cold 100% acetone for 10 min, then allowed to air dry. One section from each specimen was stained with Mayer's haematoxylin and eosin and the remaining sections were used for immunohistochemistry. Primary antibodies against Ki67 (1:1000 dilution, frozen sections, Abcam, Cambridge, UK), ghrelin (1:1000 dilution

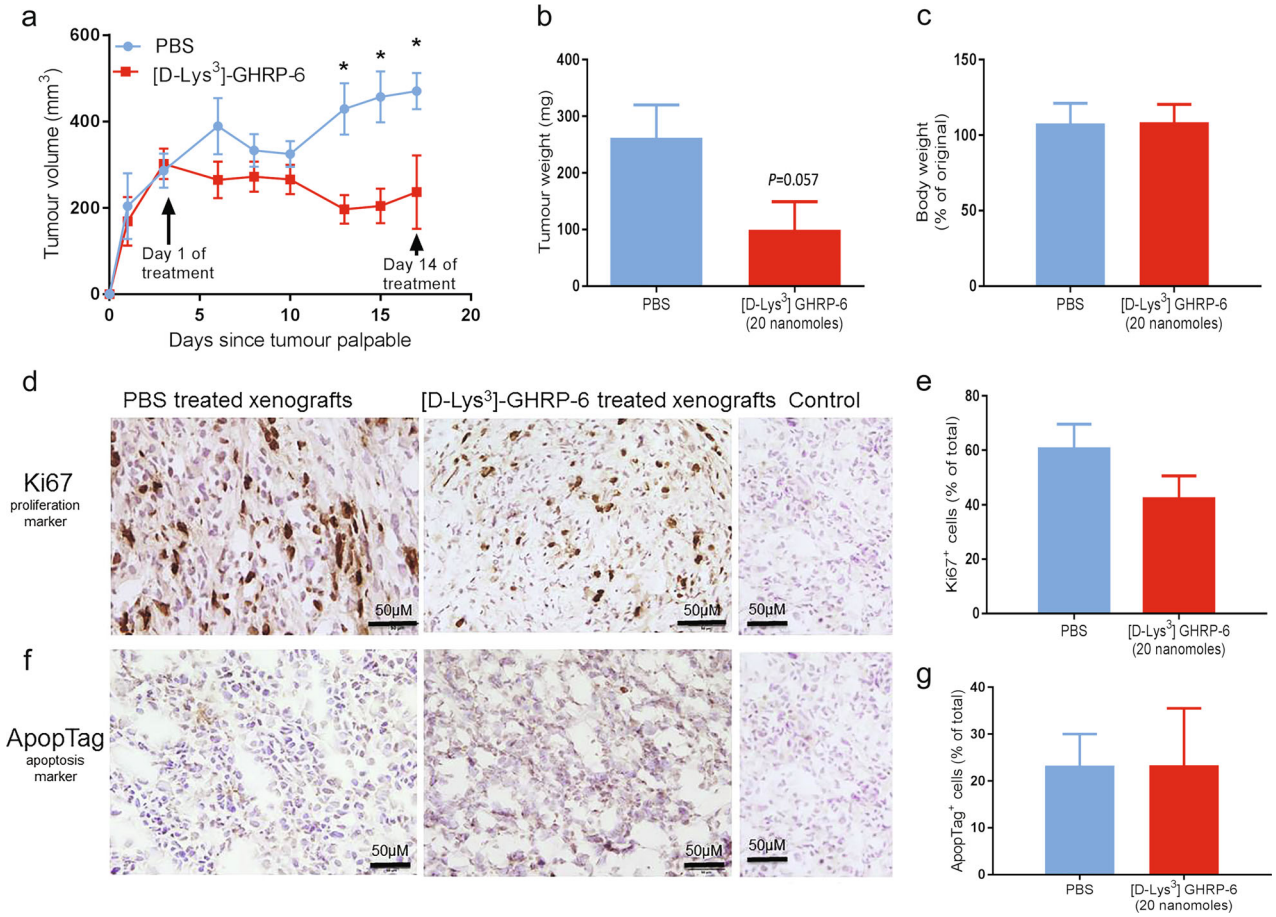

Fig. 1 [D-Lys^3]-GHRP-6 reduces PC3 tumour xenograft size 9–14 days after the commencement of treatment. Mice with subcutaneous PC3 tumour xenografts were administered 20 nmoles/mouse/day [D-Lys^3]-GHRP-6 or PBS control via intraperitoneal injection. **a** Tumour volume (mm^3) over time was significantly lower in the group treated with [D-Lys^3]-GHRP-6 ($n = 4$) compared to the control group (PBS $n = 5$). Mean ± S.E.M. *$P \le 0.016$, Wilcoxon-signed rank test. **b** Tumour weight measured at experimental endpoint. Mean ± S.E.M. $P = 0.057$, Mann–Whitney U-test. **c** Final body weight (grams) was not significantly altered at endpoint in the [D-Lys^3]-GHRP-6 treated group compared to the PBS control group. Mean ± S.E.M. $P > 0.99$, Mann–Whitney U-test. **d** Staining of the proliferation marker Ki67 in PC3 xenograft tumours administered [D-Lys^3]-GHRP-6 or PBS control. Scale bar = 50 μM. **e** Non-significant decrease in the number of Ki67-positive, proliferating cells in xenograft tumours from mice administered [D-Lys^3]-GHRP-6. Mean ± S.E.M. $P = 0.40$, Mann–Whitney U-test. **f** There is no change in the expression of the ApopTag apoptosis marker at endpoint between the treatment and control groups (Scale bar = 50 μM) or **g** in the percent of cells undergoing apoptosis in PC3 subcutaneous xenografts. Mean ± S.E.M. $P = 0.99$, Mann–Whitney U-test

for frozen sections, 1:50 for paraffin-embedded sections, Biovision, Milpitas, CA, USA) or GHSR1a were diluted (1:1000 dilution for frozen sections, 1:100 for paraffin-embedded sections, Santa Cruz Biotechnology, Dallas, TX, USA) in 1% bovine serum albumin (BSA, Sigma Aldrich) in PBS 0.05% Tween 20 (1% BSA in PBST). Ki67 immunohistochemistry was used as a marker of cell proliferation. Sections were incubated in 3% hydrogen peroxide for 10 min, to block endogenous peroxidases, followed by 60 min blocking (1% BSA in PBST), 60 min incubation with diluted primary antibody in diluents, 30 min with secondary HRP conjugated polymeric antibody (SuperPicture; Life Technologies, Carlsbad, CA, USA), and incubation with the chromagen diaminobenzidine (Dako, Troy, MI, USA) to give brown specific staining. Apoptotic cells were stained using the ApopTag *in situ* detection kit (EMD Millipore, Billerica, MA, USA). All slides were counterstained using Mayer's haematoxylin (Sigma-Aldrich), dehydrated through an alcohol gradient and xylene, and mounted using a synthetic mounting medium (D.P.X. with Colourfast, Fronine, Thermo Fisher Scientific). Cells stained positive for Ki67 or ApopTag were quantified using the ImageJ cell counter plugin (Research Services Branch, National Institute of Health, Rockville, MD, USA) [43] with minimum $n = 3$ samples per group and $n = 5$ fields per section.

Quantitative reverse transcription polymerase chain reaction (qRT-PCR)

Complementary DNA synthesis was generated from 1 μg DNase-treated RNA using an iScript cDNA synthesis kit

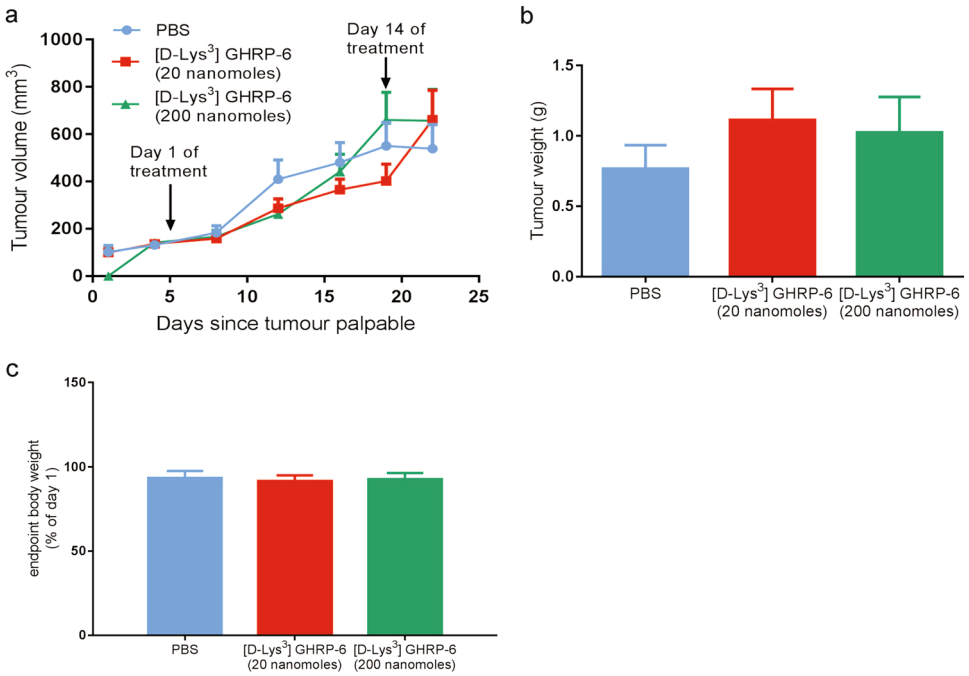

Fig. 2 The effect of [D-Lys^3]-GHRP-6 is not repeatable. NOD/SCID mice with subcutaneous PC3 tumours were administered [D-Lys^3]-GHRP-6 20 nmoles/mouse/day ($n = 11$), [D-Lys^3]-GHRP-6 200 nmoles/mouse/day ($n = 10$), or PBS control ($n = 6$) via intraperitoneal injection. **a** Tumour volume (mm^3) measured over time after commencement of [D-Lys^3]-GHRP-6 or PBS-control treatment. Mean ± S.E.M. [D-Lys^3]-GHRP-6 20 nmoles/mouse/day had no significant effect on tumour volume after 14 days treatment ($P = 0.16$), nor at endpoint (18 days) ($P = 0.96$). [D-Lys^3]-GHRP-6 (200 nmoles/mouse/day) also had no significant effect on tumour volume at 14 ($P = 0.62$) or 18 days post-treatment initiation ($P = 0.99$). Two-way ANOVA with Tukey's multiple comparisons test. **b** Tumour weight (g) measured at 18-day experimental endpoint shows no significant difference between mice administered 20 nmoles/mouse/day [D-Lys^3]-GHRP-6 ($P = 0.48$) or 200 nmoles/mouse/day [D-Lys^3]-GHRP-6 ($P = 0.71$) compared to PBS control. Mean ± S.E.M. Mann–Whitney *U*-test. **c** Percent change in body weight (grams) of mice at endpoint shows no difference between 20 nmoles/mouse/day [D-Lys^3]-GHRP-6 ($P = 0.81$) or 200 nmoles/mouse/day [D-Lys^3]-GHRP-6 ($P = 0.99$) and PBS treated mice. Mean ± S.E.M. Mann–Whitney *U*-test

(Bio-Rad, Hercules, CA, USA). Quantitative RT-PCR was performed using an AB7500 FAST sequence detection (Applied Biosystems, Foster City, CA, USA) or the ViiA 7 System (Applied Biosystems) thermal cycler. The qRT-PCR contained Applied Biosystems SYBR Green PCR Master Mix (Thermo Fisher Scientific), 1 µM each primer, and 2 µl of a 1/5 dilution of cDNA template in RNase-free water to a total volume of 10 µl. RT-PCR was performed with an annealing temperature of 60 °C for 40 cycles. A negative control (containing water instead of template) and a minus reverse transcriptase (RT) control (in which RT was omitted from the cDNA synthesis) were used for each real-time plate for each primer set. All real-time experiments were performed in triplicate, and a mean value was used for the determination of mRNA levels of epidermal growth factor receptor (*EGFR*; QT00085701, QuantiTect primer assay, QIAGEN) and the housekeeping gene TATA-box binding protein (*TBP*; F 5′-TCGCTTCCGCTGGCCCA-TAGT-3′, R 5′- TCTCCAGCACACTCTTCTCAGCAA-3′; Integrated DNA Technologies). Baseline and threshold values (C_t) for these genes were determined using ABI 7500 Prism software and exported to Microsoft Excel for analysis. The relative expression of each gene was calculated using the comparative $2^{-\Delta\Delta Ct}$ method [44].

Statistical analyses

Statistical analyses were performed using GraphPad Prism v6.01 software (GraphPad Software, San Diego, CA). Data was assessed using a two-way ANOVA with Tukey's multiple comparisons, or the nonparametric Wilcoxon-signed rank test and Mann–Whitney *U*-test. $P \le 0.05$ was considered statistically significant.

Results

[D-Lys^3]-GHRP-6 does not affect PC3 cell line proliferation in vitro

In vitro proliferation assay revealed that the PC3 cell line did not respond to [D-Lys^3]-GHRP-6 treatment for three days (0–10 µM; $P = 0.32$ and $P = 0.28$, Supplementary Fig. 1a-b).

Limited inhibition of subcutaneous PC3 xenograft growth by [D-Lys^3]-GHRP-6

The effects of [D-Lys^3]-GHRP-6 on PC3 prostate cancer cell line growth *in vivo* was investigated using a NOD/SCID mouse xenograft model. Daily intraperitoneal injections of 20 nmoles/mouse [D-Lys^3]-GHRP-6 ($n = 4$) significantly decreased tumour volume compared to PBS control ($n = 5$) after 9 ($P = 0.016$), 11 ($P = 0.012$), and 14 days (endpoint) of treatment (reduction of 50.34%, 236.63 ± 85.22 mm^3, PBS: 470.1 ± 42.0 mm^3, $P = 0.02$) (Fig. 1a). Endpoint wet tumour weight was lower in the [D-Lys^3]-GHRP-6 treated group compared to the PBS control group (Fig. 1b), however, this difference was not statistically significant ($P = 0.057$). There was no difference in mouse body weight at endpoint (Fig. 1c). No significant difference in the number of proliferative ($P = 0.40$) or apoptotic cells ($P = 0.99$) at endpoint was observed between groups (Fig. 1d–g). Immunohistochemical staining of the tumour xenografts demonstrated staining for ghrelin or the ghrelin receptor, GHSR1a, however, levels were similar for both the [D-Lys^3]-GHRP-6 treated and control tumours (Supplementary Figure 1). We next repeated the experiment with an extended treatment timeframe, beyond two weeks, as well as a higher dose of [D-Lys^3]-GHRP-6 treatments (200 nmoles/mouse/day). No statistically significant difference ($P = 0.16$) in tumour volume was observed in 20 nmoles/mouse/day [D-Lys^3]-GHRP-6 dose group at 14 days, although a decrease in tumour volume was observed (Fig. 2a). In the corresponding 18-day treatment group, no significant difference in tumour volume was observed ($P = 0.96$) (Fig. 2a). A higher dose of [D-Lys^3]-GHRP-6, 200 nmoles/mouse/day, had no significant effect on tumour volume at 14 ($P = 0.62$) or 18 days post-treatment initiation ($P = 0.99$). Similar to experiment 1, at endpoint (18 days) there was no difference in wet tumour weight or host mouse body weight compared to PBS control in the 20 nmoles/mouse/day ($P = 0.48$ and $P = 0.81$, respectively) and 200 nmoles/mouse/day ($P = 0.71$ and $P = 0.99$, respectively) group (Fig. 2b, c). Taken together, these data provide evidence of a transitory effect of the ghrelin receptor antagonist [D-Lys^3]-GHRP-6 on PC3 prostate cancer cell line xenograft tumours.

Repression of xenograft tumour EGFR expression is lost beyond two weeks of [D-Lys^3]-GHRP-6 treatment

RNA-sequencing of the PC3 xenograft tumours treated with 20 nmoles [D-Lys^3]-GHRP-6 ($n = 3$) or PBS control ($n = 3$) for 14 days (the first experiment; Fig. 1) revealed that 93 genes were differentially expressed by [D-Lys^3]-GHRP-6 (moderated *t*-test; cut-off set at fold-change ± 2.0, $P \le 0.05$)

Table 1 Differentially expressed genes by subcutaneous PC3 prostate cancer cell line xenografts in NOD/SCID mice after two-weeks of daily intraperitoneal injections of the ghrelin receptor antagonist [D-Lys^3]-GHRP-6 (20 nmoles/day/mouse) compared to PBS control

Gene name	Gene description	AbsFC	*P*-value
TNS4	Tensin 4	−3.7	0.012
MUC3A	Mucin 3A, cell surface associated	−3.7	0.009
RGL3	Ral guanine nucleotide dissociation stimulator like 3	−3.7	0.030
CXCL1	C-X-C motif chemokine ligand 1	−3.6	0.002
TUBB4A	Tubulin beta 4A class IVa	−3.6	0.008
CXCL8	C-X-C motif chemokine ligand 8	−3.6	0.007
C1orf106	Chromosome 1 open reading frame 106	−3.5	0.019
AMIGO2	Adhesion molecule with Ig like domain 2	−3.3	0.008
EEF1A2	Eukaryotic translation elongation factor 1 alpha 2	−3.2	0.005
KRT7	Keratin 7	−3.2	0.002
CLDN1	Claudin 1	−3.2	0.023
CXCL3	C-X-C motif chemokine ligand 3	−3.1	0.026
ITGB4	Integrin subunit beta 4	−3.1	0.019
SPNS2	Sphingolipid transporter 2	−3	0.037
IL6	Interleukin 6	−2.8	0.022
PDGFB	Platelet derived growth factor subunit B	−2.8	0.024
EHD2	EH domain containing 2	−2.7	0.023
SALL4	Spalt like transcription factor 4	−2.7	0.025
FOXA1	Forkhead box A1	−2.6	0.010
SORL1	Sortilin related receptor 1	−2.6	0.039
DYSF	Dysferlin	−2.6	0.021
ARHGEF16	Rho guanine nucleotide exchange factor 16	−2.6	0.035
CXCL2	C-X-C motif chemokine ligand 2	−2.5	0.020
CXCL6	C-X-C motif chemokine ligand 6	−2.5	0.002
NEDD9	Neural precursor cell expressed, developmentally down-regulated 9	−2.5	0.003
PAK6	p21 (RAC1) activated kinase 6	−2.5	0.018
NPNT	Nephronectin	−2.4	0.039
CTGF	Connective tissue growth factor	−2.4	0.001
TERT	Telomerase reverse transcriptase	−2.4	0.045
CP	Ceruloplasmin	−2.4	0.047
LSR	Lipolysis stimulated lipoprotein receptor	−2.4	0.003
PKIB	cAMP-dependent protein kinase inhibitor beta	−2.4	0.027
MAST1	Microtubule associated serine/threonine kinase 1	−2.4	0.047
PHACTR3	Phosphatase and actin regulator 3	−2.4	0.004
DKK1	Dickkopf WNT signaling pathway inhibitor 1	−2.3	0.001
MEGF6	Multiple EGF like domains 6	−2.3	0.043

Table 1 (continued)

Gene name	Gene description	AbsFC	*P*-value
SIK1	Salt inducible kinase 1	−2.3	0.005
ESRP2	Epithelial splicing regulatory protein 2	−2.3	0.024
TNFAIP3	TNF alpha induced protein 3	−2.3	0.003
CKB	Creatine kinase B	−2.3	0.006
KRT80	Keratin 80	−2.3	0.030
INHBB	Inhibin beta B subunit	−2.3	0.023
ADAMTS1	ADAM metallopeptidase with thrombospondin type 1 motif 1	−2.2	0.001
PWWP2B	PWWP domain containing 2B	−2.2	0.022
HSPA1A	Heat shock protein family A (Hsp70) member 1A	−2.2	0.001
MROH6	Maestro heat like repeat family member 6	−2.2	0.038
IGFBP5	Insulin like growth factor binding protein 5	−2.2	0.047
PRR36	Proline rich 36	−2.2	0.024
GSE1	Gse1 coiled-coil protein	−2.1	0.030
SHROOM3	Shroom family member 3	−2.1	0.041
S100P	S100 calcium binding protein P	−2.1	0.011
OXTR	Oxytocin receptor	−2.1	0.032
OSBP2	Oxysterol binding protein 2	−2.1	0.007
AFAP1	Actin filament associated protein 1	−2.1	0.012
NID2	Nidogen 2	−2.1	0.019
ADGRF1	Adhesion G protein-coupled receptor F1	−2.1	0.049
CABLES1	Cdk5 and Abl enzyme substrate 1	−2.1	0.019
FST	Follistatin	−2.1	0.008
BAIAP2L1	BAI1 associated protein 2 like 1	−2.0	0.007
DUSP5	Dual specificity phosphatase 5	−2.0	0.012
SH2D3A	SH2 domain containing 3A	−2.0	0.010
EGFR	Epidermal growth factor receptor	−2.0	0.005
LMTK2	Lemur tyrosine kinase 2	−2.0	0.015
TGM2	Transglutaminase 2	−2.0	0.018
AMOTL2	Angiomotin like 2	−2.0	0.003
NIPA1	Non imprinted in Prader-Willi/ Angelman syndrome 1	−2.0	0.014
TMEM41B	Transmembrane protein 41B	−2.0	0.013
B3GNT7	UDP-GlcNAc:betaGal beta-1,3-N-acetylglucosaminyltransferase 7	−2.0	0.004
TUFT1	Tuftelin 1	−2.0	0.043
RAD54L2	RAD54 like 2	−2.0	0.049
IL32	Interleukin 32	−2.0	0.010
MOCOS	Molybdenum cofactor sulfurase	−2.0	0.043
ARID3B	AT-rich interaction domain 3B	−2.0	0.037
SLC7A1	Solute carrier family 7 member 1	−2.0	0.036
KRT86	Keratin 86	−2.0	0.007
GPRC5A	G protein-coupled receptor class C group 5 member A	−2.0	0.021
ANO9	Anoctamin 9	−2.0	0.047
NR4A1	Nuclear receptor subfamily 4 group A member 1	−2.0	0.026
DCAF4	DDB1 and CUL4 associated factor 4	−2.0	0.007
SAMD4A	Sterile alpha motif domain containing 4A	−2.0	0.003
MISP	Mitotic spindle positioning	−2.0	0.001
ACOX2	Acyl-CoA oxidase 2	2.0	0.009
KCNK12	Potassium two pore domain channel subfamily K member 12	2.1	0.041
CA9	Carbonic anhydrase 9	2.2	0.004
C2orf82	Chromosome 2 open reading frame 82	2.3	0.002
JAKMIP1	Janus kinase and microtubule interacting protein 1	2.3	0.019
TNFRSF11B	TNF receptor superfamily member 11b	2.4	0.033
COL2A1	Collagen type II alpha 1 chain	2.5	0.041
PLA2G2A	Phospholipase A2 group IIA	2.6	0.050
KLK4	Kallikrein related peptidase 4	2.7	0.038
ZP1	Zona pellucida glycoprotein 1	2.8	0.010
MYL10	Myosin light chain 10	2.9	0.031
KRT75	Keratin 75	3.1	0.002

Absolute fold-changes (AbsFC) are indicated. Moderated *t*-test; cut-off set at fold-change ± 2.0, $P \le 0.05$

—with the majority, 81 genes, downregulated (Table 1). Gene enrichment analysis identified processes associated with chemotaxis and chemokine signalling and significant associations with lipid stimulation, cell motility, cell proliferation, and apoptosis (Table 2). To gain further insights, we interrogated the STRING database [38] to reveal protein–protein interactions between the differentially expressed genes (DEGs). Of these, 51 genes formed a distinct network (Fig. 3). Functional associations in the network were significantly enriched (expected interactions = 96, observed interactions = 223; $P \le 0.001$; see [40] for overview of statistical method). Epidermal growth factor receptor (EGFR, encoded by *EGFR*; −2.0-fold, moderated *t*-test, $P = 0.0046$) formed the centre of this network, prompting us to examine its expression in PC3 xenograft tumours that appeared to no longer respond to [D-Lys^3]-GHRP-6 treatment (the second experiment; Fig. 2). In tumours treated with 20 nmoles/mouse/day [D-Lys^3]-GHRP-6 for 18 days, qRT-PCR revealed no significant difference in *EGFR* expression (0.6 fold-change, Mann–Whitney *U*-test, $P = 0.65$) (Fig. 4).

Table 2 Gene enrichment analysis of a 51-gene network derived by STRING analysis of genes differentially expressed by subcutaneous PC3 prostate cancer cell line xenografts in NOD/SCID mice after two-weeks of daily intraperitoneal injections of the ghrelin receptor antagonist [D-Lys^3]-GHRP-6 (20 nmoles/day/mouse)

GO term_id	Proteins	Hits	*P*-value	*P*-value_fdr	Term_description
GO:0033993	729	16	4.47E-12	8.28E-09	Response to lipid
GO:0051674	761	14	1.29E-09	8.07E-07	Localization of cell
GO:0048870	762	14	1.31E-09	8.07E-07	Cell motility
GO:0060326	157	8	2.93E-09	1.35E-06	Cell chemotaxis
GO:0016477	698	13	4.88E-09	1.78E-06	Cell migration
GO:0050921	108	7	5.78E-09	1.78E-06	Positive regulation of chemotaxis
GO:0048520	127	7	1.79E-08	4.74E-06	Positive regulation of behaviour
GO:0002690	75	6	2.15E-08	4.98E-06	Positive regulation of leukocyte chemotaxis
GO:0050920	139	7	3.35E-08	6.89E-06	Regulation of chemotaxis
GO:0070098	41	5	4.04E-08	7.47E-06	Chemokine-mediated signaling pathway
GO:0002688	86	6	4.93E-08	8.29E-06	Regulation of leukocyte chemotaxis
GO:0002687	97	6	1.02E-07	1.57E-05	Positive regulation of leukocyte migration
GO:0050795	191	7	2.95E-07	4.2E-05	Regulation of behaviour
GO:0006928	1211	14	4.35E-07	5.51E-05	Movement of cell or subcellular component
GO:1901700	1214	14	4.48E-07	5.51E-05	Response to oxygen-containing compound
GO:0097305	303	8	4.76E-07	5.51E-05	Response to alcohol
GO:0030334	564	10	5.97E-07	6.22E-05	Regulation of cell migration
GO:0002685	131	6	6.05E-07	6.22E-05	Regulation of leukocyte migration
GO:0030335	324	8	7.9E-07	7.44E-05	Positive regulation of cell migration
GO:0006935	588	10	8.72E-07	7.44E-05	Chemotaxis
GO:0042330	588	10	8.72E-07	7.44E-05	Taxis
GO:0040011	1091	13	8.85E-07	7.44E-05	Locomotion
GO:2000147	333	8	9.7E-07	7.81E-05	Positive regulation of cell motility
GO:2000145	599	10	1.03E-06	7.95E-05	Regulation of cell motility
GO:0051272	338	8	1.08E-06	8.03E-05	Positive regulation of cellular component movement
GO:0040017	345	8	1.26E-06	9E-05	Positive regulation of locomotion
GO:0032103	352	8	1.47E-06	0.000101	Positive regulation of response to external stimulus
GO:0040012	647	10	2.06E-06	0.000136	Regulation of locomotion
GO:0032496	262	7	2.45E-06	0.000157	Response to lipopolysaccharide
GO:0048545	383	8	2.75E-06	0.000165	Response to steroid hormone
GO:0051270	669	10	2.78E-06	0.000165	Regulation of cellular component movement
GO:0051094	1018	12	2.86E-06	0.000165	Positive regulation of developmental process
GO:0002237	273	7	3.22E-06	0.000181	Response to molecule of bacterial origin
GO:0048729	542	9	4.02E-06	0.000219	Tissue morphogenesis
GO:0022612	105	5	4.65E-06	0.000246	Gland morphogenesis
GO:0023057	1071	12	4.82E-06	0.000248	Negative regulation of signaling
GO:0010648	1080	12	5.25E-06	0.000263	Negative regulation of cell communication
GO:0034059	2	2	5.39E-06	0.000263	Response to anoxia
GO:0043408	564	9	5.55E-06	0.000263	Regulation of MAPK cascade
GO:0060429	903	11	5.88E-06	0.000272	Epithelium development
GO:0043627	195	6	6.11E-06	0.000276	Response to oestrogen
GO:0009617	430	8	6.45E-06	0.000284	Response to bacterium
GO:0048646	914	11	6.6E-06	0.000284	Anatomical structure formation involved in morphogenesis
GO:0014070	740	10	6.79E-06	0.000286	Response to organic cyclic compound

Table 2 (continued)

GO term_id	Proteins	Hits	*P*-value	*P*-value_fdr	Term_description
GO:0042127	1344	13	8.86E-06	0.000364	Regulation of cell proliferation
GO:0032355	122	5	9.69E-06	0.00039	Response to estradiol
GO:0042325	1162	12	1.1E-05	0.000435	Regulation of phosphorylation
GO:2000026	1400	13	1.37E-05	0.00053	Regulation of multicellular organismal development
GO:0070374	132	5	1.42E-05	0.000537	Positive regulation of ERK1 and ERK2 cascade
GO:0009887	809	10	1.48E-05	0.000547	Organ morphogenesis
GO:0009888	1416	13	1.55E-05	0.000557	Tissue development
GO:0042592	1203	12	1.56E-05	0.000557	Homeostatic process
GO:0043067	1270	12	2.68E-05	0.000937	Regulation of programmed cell death
GO:0048732	385	7	3E-05	0.000999	Gland development
GO:0007229	76	4	3.02E-05	0.000999	Integrin-mediated signaling pathway
GO:0097529	76	4	3.02E-05	0.000999	Myeloid leukocyte migration
GO:0001932	1083	11	3.22E-05	0.001046	Regulation of protein phosphorylation
GO:0035295	544	8	3.51E-05	0.001103	Tube development
GO:0051241	895	10	3.52E-05	0.001103	Negative regulation of multicellular organismal process
GO:0048660	80	4	3.7E-05	0.001142	Regulation of smooth muscle cell proliferation
GO:0007435	28	3	3.81E-05	0.001156	Salivary gland morphogenesis
GO:0006954	401	7	3.89E-05	0.00116	Inflammatory response
GO:0010941	1347	12	4.79E-05	0.001406	Regulation of cell death
GO:0002009	417	7	4.98E-05	0.00144	Morphogenesis of an epithelium
GO:0007431	31	3	5.2E-05	0.00146	Salivary gland development
GO:0001101	285	6	5.21E-05	0.00146	Response to acid chemical
GO:0019220	1377	12	5.93E-05	0.001638	Regulation of phosphate metabolic process
GO:0051174	1390	12	6.5E-05	0.001768	Regulation of phosphorus metabolic process
GO:0009968	970	10	6.93E-05	0.001859	Negative regulation of signal transduction
GO:0030595	96	4	7.56E-05	0.002	Leukocyte chemotaxis
GO:0051093	789	9	7.83E-05	0.002041	Negative regulation of developmental process
GO:0048585	1202	11	8.31E-05	0.002111	Negative regulation of response to stimulus
GO:0070372	191	5	8.32E-05	0.002111	Regulation of ERK1 and ERK2 cascade
GO:0009725	802	9	8.87E-05	0.002198	Response to hormone
GO:0014910	37	3	8.91E-05	0.002198	Regulation of smooth muscle cell migration
GO:0032101	808	9	9.39E-05	0.002258	Regulation of response to external stimulus
GO:0043207	627	8	9.52E-05	0.002258	Response to external biotic stimulus
GO:0051707	627	8	9.52E-05	0.002258	Response to other organism

Obtained using the R package 'Stringdb'. Enrichment for Gene Ontology Biological Processes (GO BP) terms were computed using a hypergeometric test. The false discovery rate *P*-value is denoted as 'pvalue_fdr'

Discussion

Previous *in vitro* studies have demonstrated that the ghrelin receptor antagonist [D-Lys^3]-GHRP-6 inhibits the proliferative response to ghrelin in cultured colon [45], gastric [46], and ovarian cancer cell lines [47], human aortic endothelial cells [48], hippocampal stem cells [49], astrocytes [50], and rat [51] and human osteoblasts [51, 52]. In this study, [D-Lys^3]-GHRP-6 treatment daily over 3 days did not affect PC3 prostate cancer cell line growth *in vitro* at a range of concentrations. This could indicate that [D-Lys^3]-GHRP-6 affects tumour growth indirectly *in vivo*. Alternatively, the effects over this relatively short time course *in vitro* might not be measurable using these assays. In this study we aimed to investigate whether [D-Lys^3]-GHRP-6 had an effect on subcutaneous PC3 xenograft tumours in NOD/SCID mice. Daily injection of [D-Lys^3]-GHRP-6 reduced xenograft tumour volume after 9–14 days in an initial experiment, but had no significant effects on tumour weight or cell proliferation. In a second experiment we

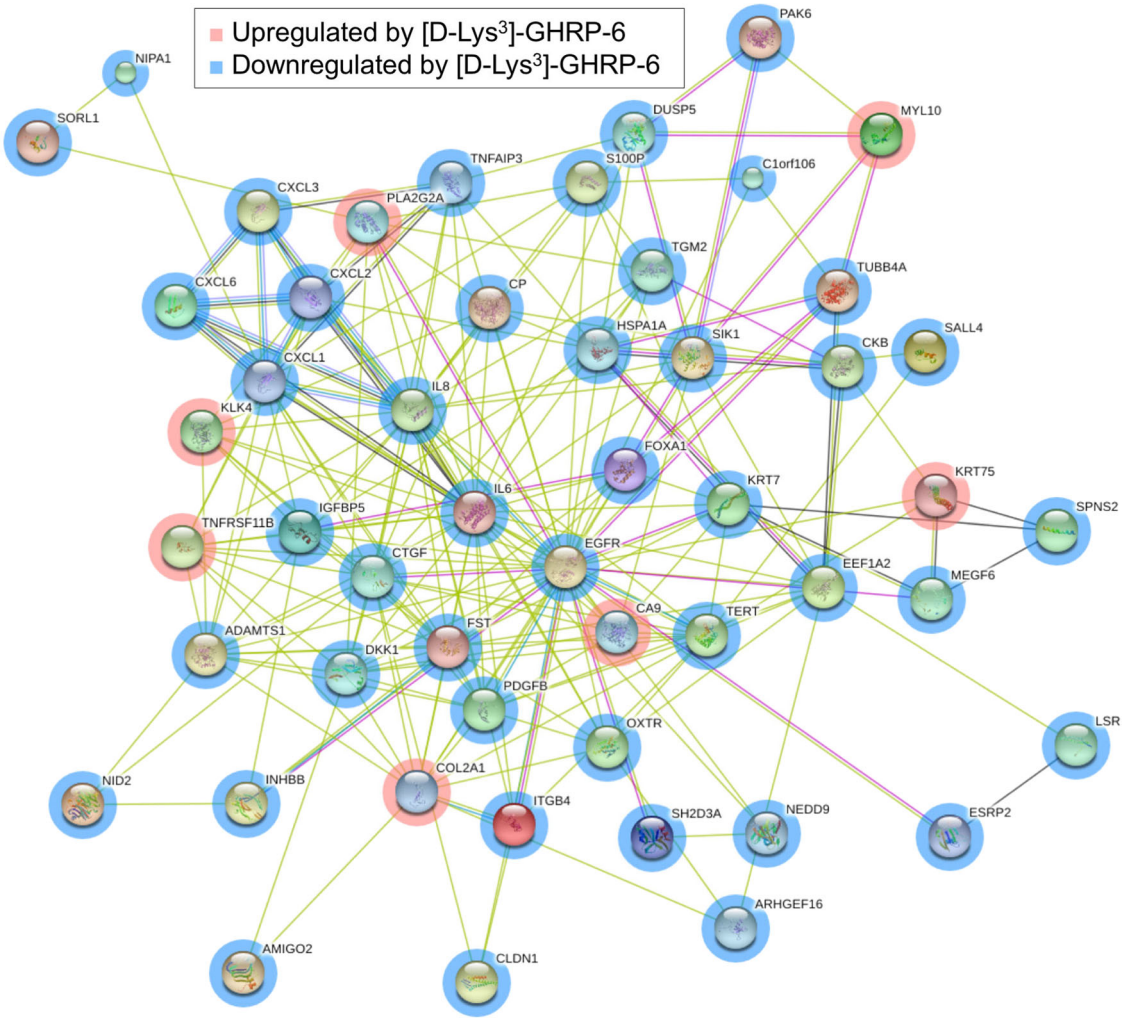

Fig. 3 STRING network consisting 51 proteins encoded by genes differentially expressed by PC3 xenograft tumours in mice administered [D-Lys^3]-GHRP-6 (20 nmoles/day/mouse) for 14 days. Genes induced (red) or repressed (blue) are indicated. 2.0-fold change and P value ≤ 0.05 cutoff

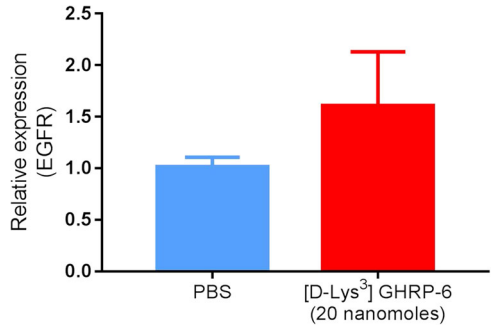

Fig. 4 Epidermal growth factor receptor (*EGFR*) expression is not significantly different in PC3 xenografts after 18 days of [D-Lys^3]-GHRP-6 treatment. Data is shown as mean ± S.E.M. ([D-Lys^3]-GHRP-6 $n = 7$; PBS control $n = 4$). Mann–Whitney U-test ($P = 0.65$)

extended the treatment regime to 18 days, revealing that the effect of [D-Lys^3]-GHRP-6 is lost after approximately two weeks of treatment. Similarly, an increased dose (200 nmoles/mouse/day) of [D-Lys^3]-GHRP-6 had no significant effect on measures of tumour growth (tumour volume and tumour weight) at 18 days.

Given the lack of data on [D-Lys^3]-GHRP-6 and prostate cancer, it is of interest to consider the literature on this antagonist in animal models. Very rapid response to ghrelin receptor antagonists, followed by resistance to treatment has previously been described [13, 46, 53]. [D-Lys^3]-GHRP-6 (~370 nmoles/mouse delivered by injection) decreased ethanol and water intake in male C57BL/6 mice, however, this effect was only seen for the first day of treatment, suggesting that [D-Lys^3]-GHRP-6 tolerance developed quickly [13]. The *Snord116* deletion mouse, a single-gene knockout model of Prader-Willi syndrome with supraphysiological levels of ghrelin, exhibited desensitisation to the anorexigenic effect of [D-Lys^3]-GHRP-6 (~336 nmoles/mouse delivered by injection) or the GHSR1a antagonist YIL-781 after 1–2 days [53]. Such rapid systemic responses

to ghrelin antagonists may be unusual, however. A recent study revealed that [D-Lys^3]-GHRP-6 inhibited ghrelin gene (*GHRL*) overexpression-mediated growth of SGC7901 human gastric carcinoma cell line xenograft tumours in nude (*Foxn1^{nu}*) mice, while the growth of untransfected SGC7901 xenografts was not significantly altered by [D-Lys^3]-GHRP-6 [46]. In the SGC7901 xenograft study 40 nmoles/mouse [D-Lys^3]-GHRP-6 was administered i.p. three times over 7 days (in our study we administered 20 or 200 nmoles/mouse i.p. daily for 14–18 days). Thus, longer-term treatment would be expected to antagonise the effects of ghrelin produced by tumours.

As GHSR1a is a GPCR, it is likely to be rapidly internalised and its effects attenuated [54] after the administration of [D-Lys^3]-GHRP-6, which may reflect the initial xenograft tumour response observed in our study and by others [46]. A number of metabolic studies have employed [D-Lys^3]-GHRP-6 short term, demonstrating its beneficial effects in obese mice and suggesting that the antagonist might be a useful treatment for type 2 diabetes mellitus [55, 56]. [D-Lys^3]-GHRP-6 (200 nmoles/mouse) decreased food intake and weight gain in the leptin-deficient (*Lep^{ob}*; *ob/ob*) mouse when they were treated twice-daily for 6 days [55]. Recently, a 12-day mouse study revealed that [D-Lys^3]-GHRP-6 treatment increased food intake and lead to impaired glucose tolerance in male, non-obese, diabetic MKR mice (a transgenic strain with skeletal muscle-specific deletion of the *Igfr1* gene), but not in the wild-type strain (FVB/NJ) [55], suggesting that the observed effects are a peculiarity of the MKR strain. Indeed, similar to wild-type FVB/NJ mice, we did not observe impaired weight gain mice in our 18-day study in NOD/SCID mice (20 or 200 nmoles/mouse daily in our study versus 200 nmoles/mouse twice a day in the previous study) [56].

To gain insight into how [D-Lys^3]-GHRP-6 was able to inhibit PC3 xenograft tumour growth in our first experiment, we performed RNA-sequencing. Of the 93 genes that were differentially regulated after 14 days of treatment with [D-Lys^3]-GHRP-6, reduced gene expression of epidermal growth factor receptor (EGFR) was of particular interest as it formed the centre of a protein–protein interaction network. After 18 days of [D-Lys^3]-GHRP-6 treatment there was no change in xenograft *EGFR* expression and growth. Abnormal activation and upregulation of EGFR is associated with aggressiveness and poor prognosis in many cancers, rendering it a promising therapeutic target [57]. EGFR regulates cell proliferation [58], and its upregulation in prostate cancer has been associated with androgen independence [59] and more aggressive, metastatic disease [60].

While we observed a significantly reduced tumour volume at 14 days in 20 nmol [D-Lys^3]-GHRP-6 treated xenografts in the first experiment, there was a slightly but not significantly lower number of cells expressing the proliferation marker Ki67 and a weaker overall immunohistochemical staining compared to PBS controls. This may be due to the development of resistance to 20 nmol [D-Lys^3]-GHRP-6 beginning around 14 days, therefore, affecting the percent of proliferating cells at this timepoint, with perhaps a significant reduction in proliferation at earlier time points. Ghrelin can transactivate EGFR, which may mediate its proliferative effects [53, 61]. This response tends to be very rapid and transient, however [62] and the effects of ghrelin on EGFR are likely to be acute. We speculate that the lower EGFR gene expression after 14 days of 20 nmoles/mouse/day [D-Lys^3]-GHRP-6 treatment in the first experiment, followed by no difference after 18 days 20 nmoles/mouse/day [D-Lys^3]-GHRP-6 treatment in the second experiment, may be due to ghrelin transactivation of EGFR [62] promoting a short-term reduction in tumour size.

To conclude, our prostate tumour xenograft study shows that the ghrelin receptor antagonist [D-Lys^3]-GHRP-6 can inhibit *in vivo* xenograft tumour growth for two weeks, followed by an apparent resistance to the antagonist. This work also identifies EGFR as a candidate mediator of tumour growth inhibition by [D-Lys^3]-GHRP-6. Although its application is likely to be limited unless the transitory effects and apparent resistance to [D-Lys^3]-GHRP-6 can be overcome by intermittent dosing regimens or other approaches. Notwithstanding our work provides further evidence that the ghrelin axis plays a role in prostate cancer progression and supports further studies.

Acknowledgements This work was supported by the National Health and Medical Research Council Australia (grant no. 1002255 and 1059021; to L.K.C., A.C.H., P.L.J., and I.S.), the Cancer Council Queensland (grant no. 1098565; to L.K.C., A.C.H., and I.S.), the Australian Research Council (grant no DP140100249; to L.K.C. and A.C.H.), a QUT Vice-Chancellor's Senior Research Fellowship (to I.S.), the Movember Foundation and the Prostate Cancer Foundation of Australia through a Movember Revolutionary Team Award, the Australian Government Department of Health, and the Australian Prostate Cancer Research Center, Queensland (L.K.C., A.C.H., and C.C.N.).

Compliance with ethical standards

Conflict of interest The authors declare that they have no conflict of interest.

Ethical approval Ethical approval was granted from the University of Queensland and Queensland University of Technology Animal Ethics Committees (TRI/QUT/087/14/NHMRC).

References

1. A.M. Wren, L.J. Seal, M.A. Cohen, A.E. Brynes, G.S. Frost, K.G. Murphy, W.S. Dhillo, M.A. Ghatei, S.R. Bloom, Ghrelin enhances appetite and increases food intake in humans. J. Clin. Endocrinol. Metab. **86**(12), 5992 (2001)

2. M. Tschöp, R. Wawarta, R.L. Riepl, S. Friedrich, M. Bidlingmaier, R. Landgraf, C. Folwaczny, Post-prandial decrease of circulating human ghrelin levels. J. Endocrinol. Invest. **24**(6), RC19–RC21 (2001)
3. M. Kojima, H. Hosoda, Y. Date, M. Nakazato, H. Matsuo, K. Kangawa, Ghrelin is a growth-hormone-releasing acylated peptide from stomach. Nature **402**(6762), 656–660 (1999). https://doi.org/10.1038/45230
4. M. Tschöp, D.L. Smiley, M.L. Heiman, Ghrelin induces adiposity in rodents. Nature **407**(6806), 908–913 (2000)
5. S.M. Abdel-Hakim, M.Y. Ibrahim, H.M. Ibrahim, M.M. Ibrahim, The effect of ghrelin antagonist (D-Lys^3) GHRP-6 on ovariectomy-induced obesity in adult female albino rats. Endocr. Regul. **48**(3), 126–134 (2014)
6. G. Xu, Z. Wang, Y. Li, Z. Li, H. Tang, J. Zhao, X. Xiang, L. Ding, L. Ma, F. Yuan, J. Fei, W. Wang, N. Wang, Y. Guan, C. Tang, M. Mulholland, W. Zhang, Ghrelin contributes to derangements of glucose metabolism induced by rapamycin in mice. Diabetologia **55**(6), 1813–1823 (2012)
7. J.N.T. Fung, P.L. Jeffery, J.D. Lee, I. Seim, D. Roche, A. Obermair, L.K. Chopin, C. Chen, Silencing of ghrelin receptor expression inhibits endometrial cancer cell growth *in vitro* and *in vivo*. Am. J. Physiol. Endocrinol. Metab. **305**(2), E305–E313 (2013)
8. L.K. Chopin, I. Seim, C.M. Walpole, A.C. Herington, The ghrelin axis--does it have an appetite for cancer progression? Endocr. Rev. **33**(6), 849–891 (2012)
9. P.L. Seim, L. Jeffery, C.M. de Amorim, J. Walpole, E.J. Fung, R. Whiteside, A.C. Lourie, L.K. Herington, Chopin, Ghrelin O-acyltransferase (GOAT) is expressed in prostate cancer tissues and cell lines and expression is differentially regulated in vitro by ghrelin. Reprod. Biol. Endocrinol. 11(1)70.1-70.9 (2013)
10. P.L. Jeffery, A.C. Herington, L.K. Chopin, Expression and action of the growth hormone releasing peptide ghrelin and its receptor in prostate cancer cell lines. J. Endocrinol. **172**(3), R7–R11 (2002)
11. I. Seim, A.A. Lubik, M.L. Lehman, N. Tomlinson, E.J. Whiteside, A.C. Herington, C.C. Nelson, L.K. Chopin, Cloning of a novel insulin-regulated ghrelin transcript in prostate cancer. J. Mol. Endocrinol. **50**(2), 179–191 (2013)
12. D. Wacker, R.C. Stevens, B.L. Roth, How ligands illuminate GPCR molecular pharmacology. Cell **170**(3), 414–427 (2017)
13. J.L. Gomez, A.E. Ryabinin, The effects of ghrelin antagonists [D-Lys(3)]-GHRP-6 or JMV2959 on ethanol, water, and food intake in C57BL/6J mice. Alcohol Clin. Exp. Res **38**(9), 2436–2444 (2014)
14. A. Moulin, L. Demange, G. Bergé, D. Gagne, J. Ryan, D. Mousseaux, A. Heitz, D. Perrissoud, V. Locatelli, A. Torsello, J.-C. Galleyrand, J.-A. Fehrentz, J. Martinez, Toward potent ghrelin receptor ligands based ontrisubstituted 1,2,4-triazole structure. 2. synthesis and pharmacological *in vitro* and *in vivo* evaluations. J. Med. Chem. **50**(23), 5790–5806 (2007)
15. S.H. Lockie, T. Dinan, A.J. Lawrence, S.J. Spencer, Z.B. Andrews, Diet-induced obesity causes ghrelin resistance in reward processing tasks. Psychoneuroendocrinology **62**, 114–120 (2015)
16. D.I. Briggs, Z.B. Andrews, Metabolic status regulates ghrelin function on energy homeostasis. Neuroendocrinology **93**(1), 48–57 (2011)
17. C.B. Steele, C.C. Thomas, S.J. Henley, G.M. Massetti, D.A. Galuska, T. Agurs-Collins, M. Puckett, L.C. Richardson, Richardson Vital signs: Trends in incidence of cancers associated with overweight and obesity — United States, 2005–2014 MMWR. Morbid Mortal Wkly Rep **66**(39), 1052–1058 (2017)
18. J. Ma, H. Li, E. Giovannucci, L. Mucci, W. Qiu, P.L. Nguyen, J. M. Gaziano, M. Pollak, M.J. Stampfer, Prediagnostic body-mass index, plasma C-peptide concentration, and prostate cancer-specific mortality in men with prostate cancer: A long-term survival analysis. Lancet Oncol. **9**(11), 1039–1047 (2008)
19. Continuous update project report. Food, nutrition, physical activity, and the prevention of breast cancer. In: Research, World Cancer Research Fund/American Institute for Cancer Research Continuous Update Project. (ed.). London: WCRF International, (2010)
20. Continuous update project report. Food, nutrition, physical activity, and the prevention of endometrial cancer. In: Research, World Cancer Research Fund/American Institute for Cancer Research Continuous Update Project. (ed.). London: WCRF International, (2013)
21. Continuous update project report. Food, nutrition, physical activity, and the prevention of colorectal cancer. In: Research, World Cancer Research Fund/American Institute for Cancer Research Continuous Update Project. (ed.). London: WCRF International, (2011)
22. B. Holst, N.D. Holliday, A. Bach, C.E. Elling, H.M. Cox, T.W. Schwartz, Common structural basis for constitutive activity of the ghrelin receptor family. J. Biol. Chem. **279**(51), 53806–53817 (2004)
23. D. Srisai, T.C. Yin, A.A. Lee, A.A.J. Rouault, N.A. Pearson, J.L. Grobe, J.A. Sebag, MRAP2 regulates ghrelin receptor signaling and hunger sensing. Nat. Commun. **8**(1), 713 (2017)
24. R.G. Smith, K. Cheng, W.R. Schoen, S.S. Pong, G. Hickey, T. Jacks, B. Butler, W.W.S. Chan, L.Y.P. Chaung, F. Judith, J. Taylor, M.J. Wyvratt, M.H. Fisher, A nonpeptidyl growth hormone secretagogue. Science **260**(5114), 1640–1643 (1993)
25. K. Patel, V.D. Dixit, J.H. Lee, J.W. Kim, E.M. Schaffer, D. Nguyen, D.D. Taub, Identification of ghrelin receptor blocker, D-[Lys3] GHRP-6 as a CXCR4 receptor antagonist. Int J. Biol. Sci. **8**(1), 108–117 (2012)
26. K. Patel, V.D. Dixit, J.H. Lee, J.W. Kim, E.M. Schaffer, D. Nguyen, D.D. Taub, The GHS-R blocker D-[Lys3] GHRP-6 serves as CCR5 chemokine receptor antagonist. Int J. Med. Sci. **9**(1), 51–58 (2012)
27. E. Van der Meer, P.L.P. Van Loo, V. Baumans, Short-term effects of a disturbed light-dark cycle and environmental enrichment on aggression and stress-related parameters in male mice. Lab Anim. **38**(4), 376–83 (2004)
28. H. Moon, J.E. Ruelcke, E. Choi, L.J. Sharpe, Z.D. Nassar, H. Bielefeldt-Ohmann, M.-O. Parat, A. Shah, M. Francois, K.L. Inder, A.J. Brown, P.J. Russell, R.G. Parton, M.M. Hill, Diet-induced hypercholesterolemia promotes androgen-independent prostate cancer metastasis via IQGAP1 and caveolin-1. Oncotarget **6**(10), 7438–7453 (2015)
29. T. Conway, J. Wazny, A. Bromage, M. Tymms, D. Sooraj, E.D. Williams, B. Beresford-Smith, Xenome--a tool for classifying reads from xenograft samples. Bioinformatics **28**, i172–i178 (2012)
30. D. Kim, G. Pertea, C. Trapnell, H. Pimentel, R. Kelley, S.L. Salzberg, TopHat2: accurate alignment of transcriptomes in the presence of insertions, deletions and gene fusions. Genome Biol. **14**(4), R36 (2013)
31. Y. Liao, G.K. Smyth, W. Shi, FeatureCounts: An efficient general purpose program for assigning sequence reads to genomic features. Bioinformatics **30**(7), 923–930 (2014)
32. M.D. Robinson, A. Oshlack, A scaling normalization method for differential expression analysis of RNA-seq data. Genome Biol. **11**(3), R25 (2010)
33. M.D. Robinson, D.J. McCarthy, G.K. Smyth, EdgeR: A Bioconductor package for differential expression analysis of digital gene expression data. Bioinformatics **26**(1), 139–140 (2010)
34. R. Gentleman, V. Carey, W. Huber, F. Hahne: Genefilter: methods for filtering genes from microarray experiments R package version In. R package version 3.3.3 (2016)

35. M.E. Ritchie, B. Phipson, D. Wu, Y. Hu, C.W. Law, W. Shi, G.K. Smyth, limma powers differential expression analyses for RNA-sequencing and microarray studies. Nucleic Acids Res. **43**(7), e47 (2015)
36. C.W. Law, Y. Chen, W. Shi, G.K. Smyth, Voom: Precision weights unlock linear model analysis tools for RNA-seq read counts. Genome Biol. **15**(2), R29 (2014)
37. S. Durinck, P.T. Spellman, E. Birney, W. Huber, Mapping identifiers for the integration of genomic datasets with the R/Bioconductor package biomaRt. Nat. Protoc. **4**(8), 1184–1191 (2009)
38. D. Szklarczyk, J.H. Morris, H. Cook, M. Kuhn, S. Wyder, M. Simonovic, A. Santos, N.T. Doncheva, A. Roth, P. Bork, L.J. Jensen, C. von Mering, The STRING database in 2017: quality-controlled protein-protein association networks, made broadly accessible. Nucleic Acids Res. **45**(D1), D362–D368 (2017)
39. D. Szklarczyk, A. Franceschini, S. Wyder, K. Forslund, D. Heller, J. Huerta-Cepas, M. Simonovic, A. Roth, A. Santos, K.P. Tsafou, M. Kuhn, P. Bork, L.J. Jensen, C. von Mering, STRINGv10: protein-protein interaction networks, integrated over the tree of life. Nucleic Acids Res. **43**(Database issue), D447–D452 (2015)
40. A. Franceschini, D. Szklarczyk, S. Frankild, M. Kuhn, M. Simonovic, A. Roth, J. Lin, P. Minguez, P. Bork, C. von Mering, L.J. Jensen, STRINGv9.1: protein-protein interaction networks, with increased coverage and integration. Nucleic Acids Res. **41** (Database issue), D808–D815 (2013)
41. G. Csardi, T. Nepusz, The igraph software package for complex network research. Inter. Complex Syst. **1695**(5), 1–9 (2006)
42. Z. Yang, R. Algesheimer, C.J. Tessone, A comparative analysis of community detection algorithms on artificial networks. Sci. Rep. **6**, 30750 (2016)
43. S.M. Hartig, Basic image analysis and manipulation in Image. J. In Frederick, M., Ausubel, F.M., Brent, R., Kingston, R.E., Moore, D.D., Seidman, J.G., Struhl, K. (eds.) Curr. Protoc. Mol. Biol. **102** pp14.15.1-14.15.12. John Wiley & Sons, Hoboken (2013)
44. K.J. Livak, T.D. Schmittgen, Analysis of relative gene expression data using real-time quantitative PCR and the 2(-Delta Delta C(T)) Method. Methods **25**(4), 402–408 (2001)
45. G.S. Lien, C.H. Lin, Y.L. Yang, M.S. Wu, B.C. Chen, Ghrelin induces colon cancer cell proliferation through the GHS-R, Ras, PI3K, Akt, and mTOR signaling pathways. Eur. J. Pharmacol. **776**, 124–131 (2016)
46. C. Tian, L. Zhang, D. Hu, J. Ji, Ghrelin induces gastric cancer cell proliferation, migration, and invasion through GHS-R/NF-kappaB signaling pathway. Mol. Cell Biochem. **382**(1-2), 163–172 (2013)
47. R.X. Bai, W.P. Wang, P.W. Zhao, C.B. Li, Ghrelin attenuates the growth of HO-8910 ovarian cancer cells through the ERK pathway. Braz. J. Med. Biol. Res. **49**(3) (2016). http://dx.doi.org/10.1590/1414-431X20155043
48. F. Rossi, A. Castelli, M.J. Bianco, C. Bertone, M. Brama, V. Santiemma, Ghrelin induces proliferation in human aortic endothelial cells via ERK1/2 and PI3K/Akt activation. Peptides **29**(11), 2046–2051 (2008)
49. H. Chung, E. Li, Y. Kim, S. Kim, S. Park, Multiple signaling pathways mediate ghrelin-induced proliferation of hippocampal neural stem cells. J. Endocrinol. **218**(1), 49–59 (2013)
50. E. Baquedano, J.A. Chowen, J. Argente, L.M. Frago, Differential effects of GH and GH-releasing peptide-6 on astrocytes. J. Endocrinol. **218**(3), 263–274 (2013)
51. N. Fukushima, R. Hanada, H. Teranishi, Y. Fukue, T. Tachibana, H. Ishikawa, S. Takeda, Y. Takeuchi, S. Fukumoto, K. Kangawa, K. Nagata, M. Kojima, Ghrelin directly regulates bone formation. J. Bone Miner. Res **20**, 790–798 (2005)
52. D.H. Wang, Y.S. Hu, J.J. Du, Y.Y. Hu, W.D. Zhong, W.J. Qin, Ghrelin stimulates proliferation of human osteoblastic TE85 cells via NO/cGMP signaling pathway. Endocrine **35**(1), 112–117 (2009)
53. D. Lin, Q. Wang, H. Ran, K. Liu, Y. Wang, J. Wang, Y. Liu, R. Chen, Y. Sun, R. Liu, F. Ding, Abnormal response to the anorexic effect of GHS-R inhibitors and exenatide in male Snord116 deletion mouse model for Prader-Willi syndrome. Endocrinology **155**(7), 2355–2362 (2014)
54. K. Howick, B. Griffin, J. Cryan, H. Schellekens, From Belly to Brain: Targeting the ghrelin receptor in appetite and food intake regulation. Int J. Mol. Sci. **18**(2), 273 (2017)
55. A. Asakawa, A. Inui, T. Kaga, G. Katsuura, M. Fujimiya, M.A. Fujino, M. Kasuga, Antagonism of ghrelin receptor reduces food intake and body weight gain in mice. Gut **52**(7), 947–952 (2003)
56. R. Mosa, L. Huang, H. Li, M. Grist, D. LeRoith, C. Chen, Long-term treatment with the ghrelin receptor antagonist [D-Lys3]-GHRP-6 does not improve glucose homeostasis in nonobese diabetic MKR mice. Am. J. Physiol. Regul. Integr. Comp. Physiol. **314**(1), R71–r83 (2018)
57. J. Mendelsohn, J. Baselga, Status of epidermal growth factor receptor antagonists in the biology and treatment of cancer. J. Clin. Oncol. **21**(14), 2787–2799 (2003)
58. J.R. Grandis, A. Chakraborty, M.F. Melhem, Q. Zeng, D.J. Tweardy, Inhibition of epidermal growth factor receptor gene expression and function decreases proliferation of head and neck squamous carcinoma but not normal mucosal epithelial cells. Oncogene **15**, 409 (1997)
59. A.M. Traish, A. Morgentaler, Epidermal growth factor receptor expression escapes androgen regulation in prostate cancer: a potential molecular switch for tumour growth. Br. J. Cancer **101** (12), 1949–1956 (2009)
60. Y. Gan, C. Shi, L. Inge, M. Hibner, J. Balducci, Y. Huang, Differential roles of ERK and Akt pathways in regulation of EGFR-mediated signaling and motility in prostate cancer cells. Oncogene **29**, 4947 (2010)
61. Y. Huang, Y. Chang, X. Wang, J. Jiang, S.J. Frank, Growth hormone alters epidermal growth factor receptor binding affinity via activation of extracellular signal-regulated kinases in 3T3-F442A cells. Endocrinology **145**(7), 3297–3306 (2004)
62. T. Waseem, M. Duxbury, S.W. Ashley, M.K. Robinson, Ghrelin promotes intestinal epithelial cell proliferation through PI3K/Akt pathway and EGFR trans-activation both converging to ERK 1/2 phosphorylation. Peptides **52**(Supplement C), 113–121 (2014)